

## Spatial Distribution and Public Health Implications of Radon and Thoron in Groundwater: A Large-Scale Study in Largest Province of Iran - 2023

Moazameh Esfandiarpour<sup>1,2</sup>, Mohammad Hassan Ehrampoush<sup>1</sup>, Fahimeh Teimouri<sup>1\*</sup>, Reyhane Sefidkar<sup>3</sup>,  
Mojtaba Rahimi<sup>4</sup>, Rohollah Fallah Madvari<sup>5</sup>, Hossein Sharifi Nejad<sup>6</sup>

<sup>1</sup> Environmental Sciences and Technology Research Center, Department of Environmental Health Engineering, School of Public Health, Shahid Sadoughi University of Medical Sciences, Yazd, Iran.

<sup>2</sup> Student Research Committee, Shahid Sadoughi University of Medical Sciences, Yazd, Iran.

<sup>3</sup> Center for Healthcare Data Modeling, Departments of Biostatistics and Epidemiology, School of Public Health, Shahid Sadoughi University of Medical Sciences, Yazd, Iran.

<sup>4</sup> Department of Physics, Faculty of Basic Science, Vali-e-Asr University of Rafsanjan, Rafsanjan, Iran.

<sup>5</sup> Department of Occupational Health Engineering, School of Public Health, Shahid Sadoughi University of Medical Sciences, Yazd, Iran.

<sup>6</sup> Regional Water Company of Kerman Province, Kerman, Iran.

### ARTICLE INFO

#### ORIGINAL ARTICLE

#### Article History:

Received: 15 May 2025

Accepted: 20 July 2025

#### \*Corresponding Author:

Fahimeh Teimouri

Email:

f.teimouri@ssu.ac.ir

Tel:

+98 35 31492151

#### Keywords:

Radioactivity;

Public Health;

Radiation Protection;

Human Body.

### ABSTRACT

**Introduction:** Radon ( $^{222}\text{Rn}$ ) and thoron ( $^{220}\text{Rn}$ ) are radioactive gases that pose significant health risks, including lung cancer, when inhaled or ingested. This study aimed to assess the health risks associated with radon and thoron in groundwater across Kerman Province, the largest province in Iran.

**Materials and Methods:** A total of 107 wells were sampled (2023), and radon/thoron concentrations were measured using a RAD7 detector. Data were analyzed using SPSS-26 and ArcMap 10.5, employing the Kruskal-Wallis test and ordinary kriging for spatial distribution mapping.

**Results:** The annual effective dose of radon ranged from  $10.00 \pm 6.72$  to  $224.84 \pm 28.40$   $\mu\text{Sv/yr}$  for adults, while thoron doses ranged from  $15.00 \pm 10.07$  to  $337.26 \pm 42.59$   $\mu\text{Sv/yr}$  for adults. No significant correlation was found between radon concentration and environmental parameters (pH, temperature, and residual free chlorine). Seven sampling points exhibited a high respiratory risk, whereas the others posed a moderate risk. No association was observed between the radon/thoron levels and fault proximity.

**Conclusion:** All measured radon concentrations were below Iran's permissible limit (100 Bq/L). To mitigate health risks, high-concentration wells should be restricted or sealed, and aeration/storage tanks ( $\leq 4$ -day retention time) should be implemented to reduce radioactivity. These measures are crucial for minimizing public exposure to radioactive groundwater contamination.

**Citation:** Esfandiarpour M, Ehrampoush MH, Teimouri F, et al. *Spatial Distribution and Public Health Implications of Radon and Thoron in Groundwater: A Large-Scale Study in Largest Province of Iran - 2023*. J Environ Health Sustain Dev. 2025; 10(3): 2746-56.

### Introduction

Radon ( $^{222}\text{Rn}$ ) is a dense radioactive gas released from the decay of radium in soil, rocks, and water, which then seeps into the air<sup>1</sup>. Both radon and thoron gases emit high-energy alpha particles, which have been historically linked to

fatal lung diseases in miners since the 16th century<sup>1</sup>. Alpha particles from radon decay are a form of ionizing radiation that can damage living cells, potentially causing them to become cancerous through uncontrolled replication<sup>2</sup>.

The first comprehensive study on the

relationship between radon exposure and lung cancer risk in underground miners was the Biological Effects of Ionizing Radiation (BEIR) IV report, which included cohort studies of miners in Colorado, Ontario, Eldorado, and Malmberget<sup>3</sup>. A single alpha particle can cause extensive DNA damage and genetic mutations in a cell, potentially leading to cancer or physical defects in a developing fetus, which can affect future generations<sup>3</sup>. Research confirms that radon is dangerous even at low levels, as its alpha particles can indirectly damage DNA by creating cell-damaging chemical radicals without directly hitting the nucleus, indicating that there is no safe threshold for exposure.

Due to its high concentration and the long-lived hazard of its decay product,  $^{212}\text{Pb}$ , measuring  $^{220}\text{Rn}$  (thoron) in drinking water is critically important, as it is a major source of exposure in nearby locations<sup>4</sup>. Areas with radium-rich geology, such as granite, have a high likelihood of elevated  $^{222}\text{Rn}$  levels in local water sources, posing both inhalation and ingestion radiation risks.

As  $^{222}\text{Rn}$  dissolves easily in water, it can be easily separated from water by exposure to air or stirring<sup>5</sup>. Consequently, it is vital to measure the dose of natural and synthetic radioactive elements in the environment and study their health effects, which is why most countries continuously report radiation measurements<sup>6</sup>. According to health and environmental standards, the safe limit for radon-222 ( $^{222}\text{Rn}$ ) concentration in drinking water is 11 Bq/L, with an annual effective dose limit of 100  $\mu\text{Sv/yr}$ <sup>5</sup>.

Various studies have investigated the relationship between high concentrations of  $^{222}\text{Rn}$  gas and the technological status of various regions. For example, Jamir et al. (2023) estimated groundwater and soil  $^{222}\text{Rn}$  and  $^{220}\text{Rn}$  exhalation rates in the Mokochung district of Nagaland, India. The soil  $^{222}\text{Rn}$  concentration varied from 27

to 40  $\text{mBqKg}^{-1}\text{h}^{-1}$ , while the  $^{220}\text{Rn}$  concentration of the soil varied from 714 to 2166  $\text{Bqm}^{-2}\text{h}^{-1}$  and the  $^{222}\text{Rn}$  concentration in the groundwater ranged from 1.48 to 2.22 Bq/L<sup>6</sup>. In the Zarand region of Iran, 48% of groundwater samples exhibited radon concentrations exceeding 11 Bq/L, with values ranging from  $4.67 \pm 2.077$  to  $31.55 \pm 4.912$  Bq/L, indicating a significant correlation with geological features such as proximity to faults and water pH levels<sup>7</sup>. Similarly, in the Qassim area of Saudi Arabia, radon concentrations in groundwater samples ranged from 0.76 to 9.15 Bq/L, averaging 3.56 Bq/L, which is within the EPA's recommended limits<sup>8</sup>. In Qatar, studies have revealed radon levels between 1.5 and 23.4 Bq/L in groundwater, exceeding those reported in several other countries, highlighting the effects of regional geology on radon distribution<sup>9</sup>.

Although many studies have been conducted on  $^{222}\text{Rn}$  radioactivity (radioactivity is the act of emitting radiation, spontaneously) and health risk assessment, few studies have been conducted on the zoning of  $^{222}\text{Rn}$  gas and  $^{220}\text{Rn}$  in areas at risk of earthquakes. Given the general characteristics of Kerman Province, researchers decided to investigate the concentrations of  $^{222}\text{Rn}$  and  $^{220}\text{Rn}$  gases in the groundwater of this province from the perspective of assessing health risks. This study aimed to evaluate the health risks posed by radon and thoron in groundwater and generate a zoning map to identify high-risk areas in Kerman province, Iran.

## Material and Methods

### Study Area and Sampling Site Determination

According to the latest census in 2016, the population of Kerman Province was 3,164,718. This province is the largest in Iran, and its capital is Kerman. Kerman province constitutes more than 11% of the Iran area, with approximately 183,193 square kilometers, and is the largest province in Iran (Figure 1).

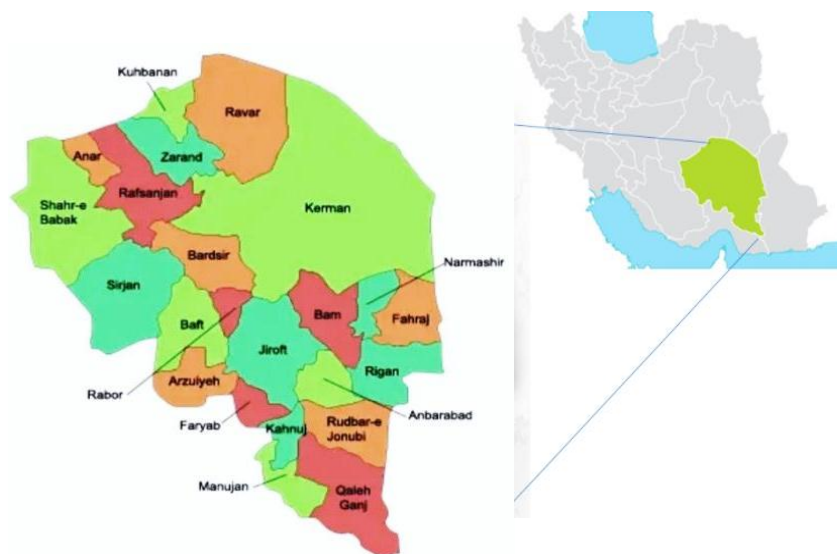


**Figure 1:** Location of Kerman province.

This province is located at an altitude of 1700–1800 meters above sea level on the northeastern edge of the Kerman Plain<sup>10</sup>. Among the 23 cities in Kerman province, 11 are in the fault zone. According to Tabnak (2024), there were 4,665 new cancer cases in Kerman Province over the past year, indicating that the rate of increase in cancer cases is higher than the national average. According to the Iranian Stem Cell Information Center report from Kerman province (2007), the second highest cancer rate among men was related to lung cancer.

Kerman province is located in the sedimentary-volcanic belt of central Iran and has various igneous rocks and geological forces in the form of tensile and compressive forces that have caused many fractures and faults in this region. For example, in Ravar City, igneous rocks are

separated into two groups: basalt and gabbro and intermediate (andesite and diorite), and in Zarand City, the entire region is covered with abundant internal mafic igneous masses, with diorite-gabbro combinations and external equivalents. These include basaltic dykes injected into the volcanic-sedimentary rocks of the Rizo series. Sirjan city contains various metamorphic rocks of igneous and sedimentary origin, such as slate, phyllite, schist, epidote, amphibolite, gneiss, quartzite, and marble. In addition, in Kerman province, geological forces in the form of tensile and compressive forces have caused many fractures and faults in this region.

In this study, 107 active drinking water wells were selected in collaboration with the Regional Water Company of the Kerman Province. The sampling locations for  $^{222}\text{Rn}$  and  $^{220}\text{Rn}$  activity measurements are shown in Figure 2.

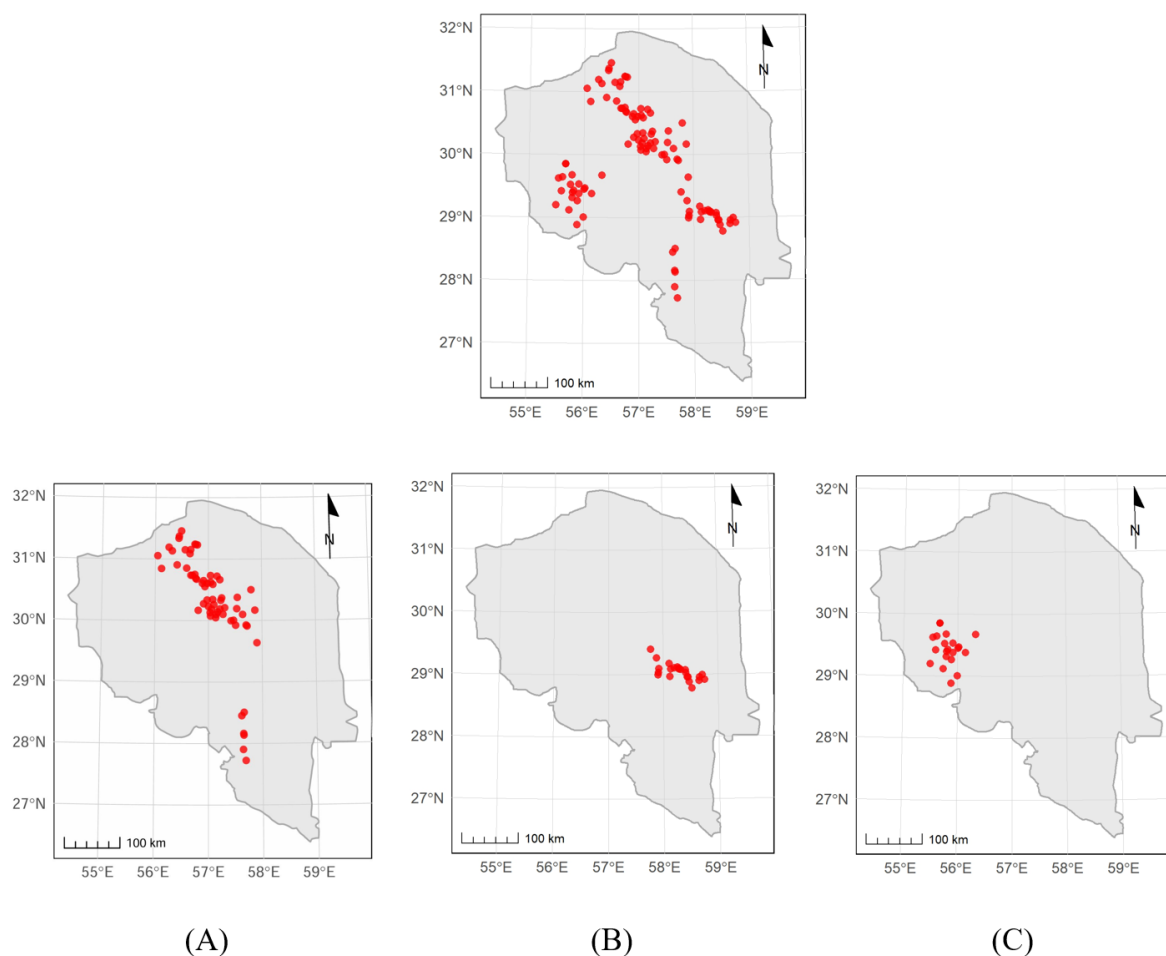


**Figure 2:** Geographical location of sampled points in Kerman province as aquifers: A- aquifer 1, B- aquifer 2 and C- aquifer c.

The well selection criteria included: (1) operational status (active wells), (2) flow rate, and (3) proximity to fault zones (<1000 m). These parameters were prioritized to assess the potential geological influences on radionuclide concentrations in groundwater sources.

#### **Water Sampling and Radioisotope (Rn-222/Rn-220) Measurement**

This study was conducted in 2023 (winter season). The RAD7 detector was used as an active method for  $^{222}\text{Rn}$  and  $^{220}\text{Rn}$  detection<sup>11</sup>. The characteristics of the RAD7 were as follows: it was manufactured by DURRIDGE Company, USA. The Mentioned device can detect  $^{222}\text{Rn}$  and thoron in water, soil, and air environments and has a printer to record the results instantly. Measurements were performed using the wat 250 protocol. The device was calibrated by the Tehran

Atomic Energy Organization. Calibration was performed with a radium-226 source of the flow type with a radioactivity of 285/107 KBq, and the radioactivity of  $^{222}\text{Rn}$  produced by this method was in the range of 140 Bq.m<sup>3</sup> -27 KBq.m<sup>3</sup>. uncertainty calibration coefficient was  $0.95 \pm 6\%$ . A 250 mL glass bottle was used for the sampling. Samples were collected once from each well; therefore, the total number of samples in this study was 107 (107 wells). Additionally, the sampling method was conducted according to the guidelines provided in the RAD7 manual (wat 250 Protocol method) using the water accessories of this device. Before the Th measurement, the necessary settings were made as follows to simultaneously measure the amount of Rn and Th: Menu--> Enter --> Setup --> Setup protocol --> enter --> Thoron --> on --> enter --> test start --> enter. Finally, the RAD7 device

counts the Rn and Th signals simultaneously with minimal interference from one to the other. RAD7 creates bubbles through a closed cycle in a period of 5 min, and during this period, approximately 94% of  $^{222}\text{Rn}$  is separated from water. After 5 min, the pump was turned off until the device reached equilibrium. After reaching equilibrium between water, air, and  $^{222}\text{Rn}$ , and the particles attached to the detector, the radioactivity of  $^{222}\text{Rn}$  was measured at 5-minute intervals. During the measurement period, alpha particles were created as a result of the decay of  $^{222}\text{Rn}$  gas and were recorded by the device. Finally, the amounts of  $^{222}\text{Rn}$  and  $^{220}\text{Rn}$  concentrations were determined<sup>12</sup>. It should be mentioned that gas measurement and detection were performed simultaneously.

#### Annual effective dose determination and health risk assessment

In the present study, the annual effective dose absorbed by drinking was calculated using the following equation:

$$E = K \cdot C \cdot KM \cdot t \quad (1)$$

In this regard, E is the effective annual dose from drinking water in Sievert per year, and K is the conversion factor of the drinking dose of  $^{222}\text{Rn}$ , which is  $10^{-8}$  for adults (people over 10 years old) and  $2 \times 10^{-8}$  Sievert per year for children (people under 10 years old). In addition, C is the concentration of  $^{222}\text{Rn}$  gas in terms of Bq per liter, KM is the amount of water consumption (average of 2 L per day for adults and 1.5 L for children), and t is the duration of consumption in the whole year, that is, 365 days.

The hazard quotient (HQ) and the Comprehensive Risk Information System (IRIS) database were used for health risk assessment estimation<sup>11-13</sup>. The basic equation for calculating the excess lifetime cancer risk is as follows:

$$\text{Risk} = \text{CDI} \times \text{SF} \quad (2)$$

Where:

Risk = a unitless probability of an individual developing cancer over their lifetime.

CDI = chronic daily intake or dose [pCi, pCi-year/g, pCi-year/L, pCi-year/m<sup>3</sup>]

SF = slope factor, expressed in [risk/pCi or risk-

g/pCi-year, risk-L/pCi-year, risk-m<sup>3</sup>/pCi-year (10):

The slope factor is the acceptable range in which there is a probability of causing a response per lifetime consumption of one unit of a chemical, and its unit is kg/d/mg.

The results obtained in the following groups, segmentation, and amount of health risk were estimated:

$$\text{CDI} = \frac{C \times (\text{RBA} \times \text{DI}) \times \text{ED} \times \text{EF}}{\text{BW} \times \text{AT}} \quad (3)$$

CDI, chronic daily absorption amount (mg/kg/day). This represents the exposure to a mass of substance per unit of body weight per unit of time over a relatively long period.

**C:** Concentration of each parameter in groundwater analysis (mg/L)

**RBA:** Relative bioavailability (no units)

**DI:** Daily intake amount (L/day)

**ED:** Exposure time ((years)

**EF:** Frequency of exposure (days/year)

**BW:** body weight (kg)

**AT:** Average time to adverse health effects (days)<sup>13, 14</sup>.

According to the values obtained from the above equation, the World Health Organization (WHO) has accepted the risk of carcinogenesis in the range between  $10^{-5}$  and  $10^{-6}$  and less than this value; While the US Environmental Protection Agency has recommended values less than  $10^{-6}$ <sup>15</sup>.

#### Statistical analysis

To describe  $^{222}\text{Rn}$  and  $^{220}\text{Rn}$  levels, median and interquartile ranges were reported. Kruskal Wallis test was also used to compare  $^{222}\text{Rn}$  and  $^{220}\text{Rn}$  levels among aquifers. Furthermore, ordinary kriging was applied to map the  $^{222}\text{Rn}$  and  $^{220}\text{Rn}$  concentrations in Kerman Province. Ordinary kriging is a geostatistical method used for spatial interpolation. Data analysis was performed using the SPSS-26 software and ArcMap 10.5.

#### Results

##### Radionuclide Activity Concentrations

The measured activity concentrations of  $^{222}\text{Rn}$  (mean  $\pm$  SD:  $9.53 \pm 12.6$  Bq/L) and  $^{220}\text{Rn}$  ( $0.91 \pm 1.98$  Bq/L) in groundwater exhibited significant spatial variability across Kerman Province (Figure 3).



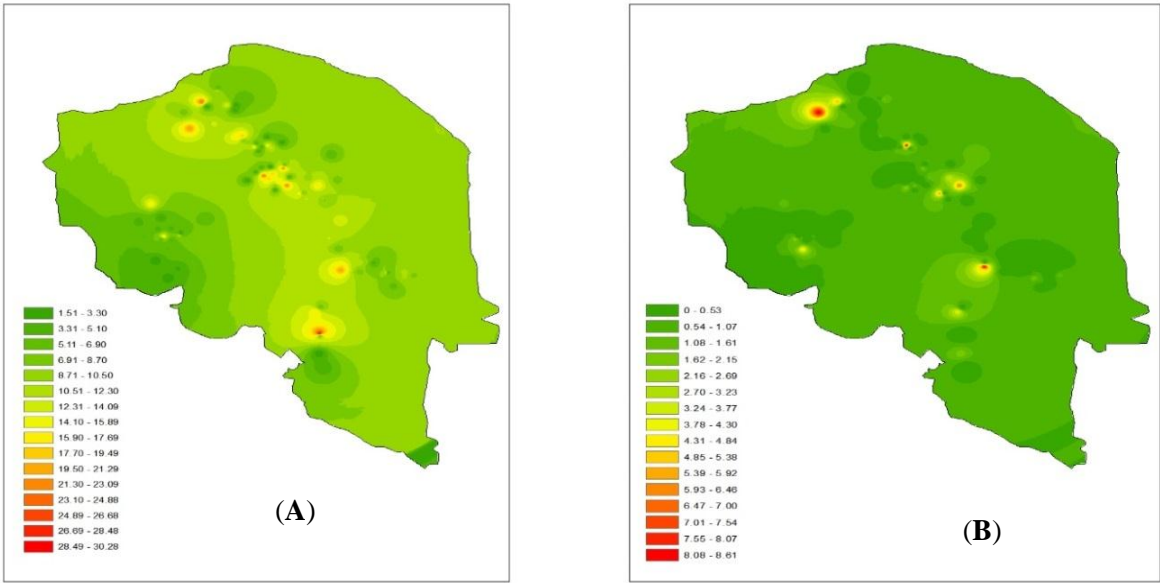


**Figure 3:** Total radon and thoron concentrations in aquifers of Kerman province (A: radon, B: thoron) as Bq/L.

Comparative analysis revealed that 64.5% of the sampled wells (n = 69) demonstrated <sup>222</sup>Rn levels below the USEPA maximum contaminant level (MCL) of 11 Bq/L. Geospatial analysis identified elevated radionuclide concentrations in three distinct regions: the central basin areas, northwestern sectors, and southeastern zones.

Notably, the northern segments of Aquifers 1 and 2 exceeded the regulatory thresholds for both isotopes (> 11 Bq/L). Statistical evaluation using

Spearman's rank correlation (ρ) showed no significant associations (p > 0.05) between <sup>222</sup>Rn activity and the measured physicochemical parameters (pH, temperature, and residual free chloride).

***Influence of Fault Zones on Radionuclide Concentrations***

Table 1 shows the values of <sup>222</sup>Rn and <sup>220</sup>Rn in the presence of faulted areas.

**Table 1:** Comparison of radon and thoron levels in different aquifers as the fault presence (Bq/l)

Non-Fault Zone Radionuclide Distribution					Fault Zone Radionuclide Distribution				
Gas	Aquifer	Number of samples	Median	Interquartile range	p	Number of samples	Median	Interquartile range	p
Radon	Aquifer 1	50	8.89	11	0.03	13	8.76	13.38	0.59
	Aquifer 2	21	8.90	5.39		2	10.60	-	
	Aquifer 3	18	5.05	3.43		3	4.39	-	
Thoron	Aquifer 1	50	0	1.34	0.75	13	0	1.53	0.65
	Aquifer 2	21	0	0.52		2	0	-	
	Aquifer 3	18	0	1.32		3	0	-	

As summarized in Table 1, measured activity concentrations of <sup>222</sup>Rn and <sup>220</sup>Rn were compared across fault-proximal and non-fault sampling sites.

Figure 4 shows the number of sampling points in the fault zone.

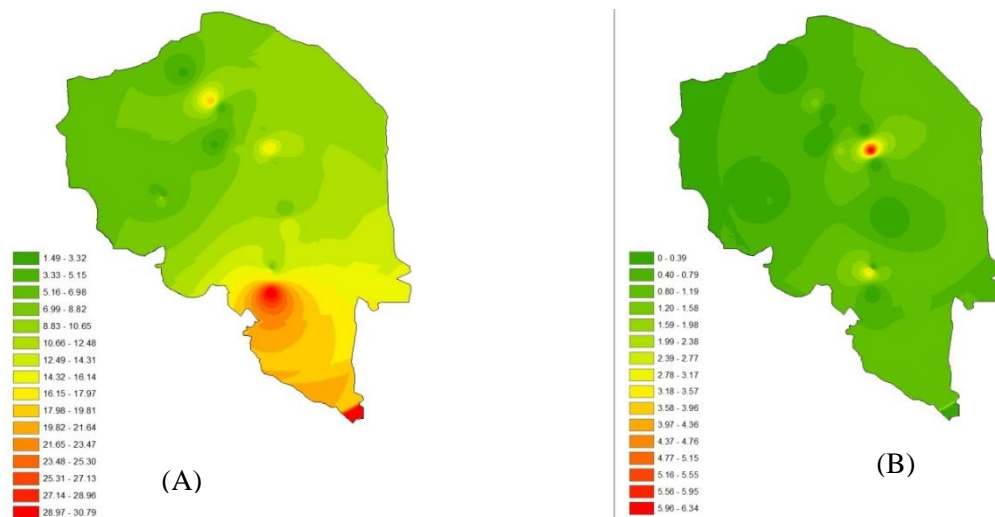


**Figure 4:** Fault Zone Influence on Groundwater Radon/Thoron Concentrations (A: radon, B: thoron) as **Bq/L**.

Spatial distribution analysis (Figure 4) revealed that  $^{222}\text{Rn}$  exhibited a broader concentration range than  $^{220}\text{Rn}$  in the fault-associated samples. In addition, 17% of the sampling points ( $n=18$ ) were located within the active fault zones. Nonparametric analysis (Mann-Whitney U test) showed no statistically significant difference in radionuclide concentrations between fault and non-fault sites: ( $^{222}\text{Rn}$ :  $p = 0.97$ , and  $^{220}\text{Rn}$ :  $p = 0.65$ ).

#### *Annual effective dose and health risk assessment*

The estimated annual effective dose from  $^{222}\text{Rn}$  ingestion was 10.00–224.84  $\mu\text{Sv/yr}$  for adults and 15.00–337.26  $\mu\text{Sv/yr}$  for children. These values substantially exceeded the WHO reference levels for radon ingestion: adult threshold:  $1.0 \times 10^{-8}$  Sv/yr (10  $\mu\text{Sv/yr}$ ) and pediatric threshold:  $2.0 \times 10^{-8}$  Sv/yr (20  $\mu\text{Sv/yr}$ ).

In the current study, the minimum and maximum values of the annual absorption dose of  $^{222}\text{Rn}$  gas for adults were 10.00 and 224.84  $\mu\text{Sv/yr}$ , and for children, they were 15.00 and 337  $\mu\text{Sv/yr}$ , respectively. It should be noted that the standard values determined by the WHO for two groups of children (under 10 years old) and adults are  $2 \times 10^{-8}$  and  $10^{-8}$  Sv/year, respectively. According to the standard values, the estimated effective dose was high in this study.

The ingestion and immersion risks associated with the selected water wells were negligible, with

calculated values below the  $1 \times 10^{-6}$  threshold. However, seven wells presented a high respiratory risk (exceeding  $1 \times 10^{-4}$ ), while the remainder were within the acceptable risk range ( $1 \times 10^{-6}$  to  $1 \times 10^{-4}$ ). However, the cumulative cancer risk range from Radon-222 and Thoron-220 exposure was  $7.76 \times 10^{-7}$ – $1.53 \times 10^{-4}$ .

#### **Discussion**

This study aimed to evaluate the human health risks associated with  $^{222}\text{Rn}$  and  $^{220}\text{Rn}$  exposure via groundwater consumption and develop a geospatial risk distribution model for Kerman Province. The findings indicate that while all measured radionuclide concentrations remained below Iran's regulatory threshold (100 Bq/L), elevated  $^{222}\text{Rn}$  levels exceeding the EPA's recommended drinking water standard (11 Bq/L) were detected at discrete sampling locations, predominantly in the central, northwestern, and southeastern regions. These spatial heterogeneities in the radon distribution may reflect variations in local hydrogeological conditions, including aquifer lithology and permeability characteristics. The consistency with other national studies validates the credibility of the findings. For example, according to Asadi et al. (2020), almost 29.54% of groundwater samples were above 11 Bq/L for  $^{222}\text{Rn}$  in Shahr Babak city<sup>5</sup>. Jahandari et al. (2012) discovered high levels at eight major sampling sites in Baft<sup>4</sup>. The highest value recorded by Mehrabi (2019) in Jiroft was

34.53 Bq/L, attributed to the presence of a volcanic belt in the region<sup>16</sup>. Rahimi et al. (2018) provided values of up to 31.55 Bq/L in Zarand<sup>17</sup>. These findings are consistent with those of the present study, where, even though the average concentrations were within acceptable limits, high-risk isolated areas became evident.

Interestingly, international data corroborate our findings. Jamir et al. (2023). For instance, measured groundwater <sup>222</sup>Rn levels in Nagaland, India, were within a range of 1.48-2.22 Bq/L, considerably less than the peaks indicated in our study, thus suggesting a relatively higher geological susceptibility of the present study area<sup>6</sup>. The consistency of the above results and their geological setting, both nationally and internationally, underlines the role of localized geological characteristics in affecting <sup>222</sup>Rn and <sup>220</sup>Rn migration into groundwater systems.

A critical observation is that some of the sampling points had an estimated effective annual dose of <sup>222</sup>Rn exceeding the standard limit of 100 µSv/yr. Children are particularly at risk in instances of this kind, as they are regarded as more sensitive to internal radiation due to their physiological characteristics, such as a higher respiratory rate and lower body mass. The limited number of sampling points near faults (16.8%) may have hindered us from assessing the contribution of these geological fractures to this outcome in detail; however, the risk remains substantial in areas devoid of faults.

The findings confirm that Rahimi et al. (2018) reported <sup>222</sup>Rn levels in the Zarand region, where both children and adults were exposed beyond the accepted level<sup>17</sup>. In addition, the same authors showed that although the annual dose for adults remained within safe limits, it grossly exceeded the limit for children<sup>5</sup>. These results suggest that commonalities in developmental and physiological factors that differ by age influence the risk levels, even when exposed to similar environmental levels.

On a global scale, Fazal Ullah et al. (2021) reported the presence of alarming levels of radiation dosages in northern Pakistani hot springs

contaminated with <sup>222</sup>Rn: 626 µSv/yr at Gilgit and 34.7 µSv/yr at Chitral, both above the recommendations of the WHO<sup>18</sup>. Similarly, Mousavi Aghdam et al. (2021) recorded annual doses as high as 1 mSv/year in southeastern Ireland, showing that this is indeed a worldwide public health issue<sup>19</sup>. Further evidence for this pattern comes from Malakootian et al. (2015), who reported that in villages close to the Rafsanjan fault, the effective annual dose in 21 children samples exceeded the recommended levels, with maximum values reaching 253.71 µSv/yr<sup>20</sup>. Negarestani et al. (2012) also showed that <sup>222</sup>Rn exposure from primary water sources in Baft City exceeded the multipliers of the safety limits<sup>21</sup>. This indicates that the increased effective dose detected in this study is not haphazard or isolated but is part of a more extensive trace observed within the country and globally, especially in areas with very distinct hydrogeological characteristics intermittently combined with potential faulting activity.

Cross-regional comparisons have demonstrated that the effective annual dose of <sup>222</sup>Rn in drinking water can range widely, from several hundred µSv/yr to values exceeding 1000 µSv/yr in extreme cases. Such variations are largely governed by geological and hydrogeological characteristics, including aquifer porosity and permeability, proximity to tectonic faults, and subterranean water flow conditions. Seasonal shifts and environmental dynamics, such as rainfall and groundwater level changes, may also affect <sup>222</sup>Rn solubility and concentration. In our study, the type and structure of the aquifer emerged as more influential factors than fault proximity in explaining the distribution of <sup>222</sup>Rn and <sup>220</sup>Rn concentrations.

This is also supported by the findings of Fakhri et al. (2015), that is, the eastern and southeastern zones of the Marand Plain are more vulnerable to contaminant intrusion<sup>22</sup>. These zones have coarser sediments and open aquifers than the other zones. The sedimentological characteristics may contribute to the movement and accumulation of <sup>222</sup>Rn gas in water sources, which represents the current spatial risk zones of the present study.



Long-term ingestion or inhalation would constitute a credible public health risk in cases where groundwater systems contain high levels of  $^{222}\text{Rn}$ . Inhalation of short-lived decay products, the most important of which are polonium-218 and polonium-214, can effectively adhere to the epithelial lining of the respiratory tract, leading to prolonged internal exposure. This scheme, as detailed by Danaei et al. (2019), provides biological plausibility for chronic tissue damage and an increased cancer risk<sup>23</sup>. In accordance with this outcome, Jafari (2016) pointed toward the rise in respiratory ailments correlated with elevated  $^{222}\text{Rn}/^{220}\text{Rn}$  levels in indoor air<sup>24</sup>.

Moreover, the likelihood of lung cancer due to  $^{222}\text{Rn}$  exposure is particularly high in smokers. In a detailed study by Shahbazi et al. (2019), the risk of lung cancer for male and female smokers exposed to  $^{222}\text{Rn}$  was 14 and 12 times higher, respectively, than that of non-smokers<sup>25</sup>. Likewise, Goli Ahmadabad et al. (2017) stated that the lifetime cancer risk associated with  $^{222}\text{Rn}$  exposure from geothermal springs in Behbahan was considerably increased, thereby supporting our findings regarding high-to-moderate immersion (recreational and hygienic water-contact activities) risk levels in certain sampling areas<sup>26</sup>.

Overall, the present findings demonstrate that while  $^{222}\text{Rn}$  and  $^{220}\text{Rn}$  concentrations at most sampling points remained within acceptable national standards, certain localized zones still pose a measurable health risk, particularly for vulnerable populations. The variation in dose levels was more closely linked to aquifer characteristics than fault proximity, suggesting the need for hydro-geologically informed monitoring strategies. These observations are in accordance with national and international evidence and highlight the importance of continuous surveillance and localized risk assessment to protect public health. However, the absence of some data, such as aquifer characterization, lithosphere type, and aquifer depth, is considered a limitation of this study.

## Conclusion

The primary objective of the present study was

to determine the concentrations of  $^{222}\text{Rn}$  and  $^{220}\text{Rn}$  in groundwater in Kerman, the largest province in Iran. The results showed that their concentrations were high in the central, northwestern, and southeastern regions of the maps. According to the maximum permissible level of radon in Iran, all the measured values were within the national standard. In addition, there was no significant relationship between gas concentrations and fault presence. However, the latter results could be related to the small sample sizes in this area. The selected points had a low risk of immersion (recreational and hygienic water-contact activities) and ingestion. However, seven points had a high respiratory risk, while the others had an acceptable respiratory risk. Radiation protection suggestions for public health include not using or sealing wells that have a high concentration of radioactive gases, using aeration tanks, and water storage tanks with a maximum retention time of 4 days to neutralize exposure to  $^{222}\text{Rn}$  and  $^{220}\text{Rn}$ .

## Acknowledgements

The authors would like to thank Shahid Sadoughi University of Medical Sciences for supporting the study.

### Conflict of Interest

The authors declare that they have no conflicts of interest.

## Funding

This work was financially supported by the Regional Water Company of Kerman Province.

## Ethical Considerations

This study was approved by the Ethics Committee of Shahid Sadoughi University of Medical Sciences (IR.SSU.SPH.REC.1401.119).

## Declaration of competing interests

The authors declare that there are no conflicts of interest in the present study.

## Author Contributions

[Fahimeh Teimouri] and [Mohammad Hassan Ehrampoush] contributed to the study conception and study design. Sampling was performed by [Moazameh Esfandiarpour] and [Hossein Sharifi Nejad]. Data collection and analysis were

performed by [Reyhane Sefidkar], [Mojtaba Rahimi] and [Rohollah Fallah Madvari]. The first draft of the manuscript was written by [Moazameh Esfandiarpour] and edited by [Fahimeh Teimouri]. All the authors have read and approved the final manuscript.

This is an Open-Access article distributed in accordance with the terms of the Creative Commons Attribution (CC BY 4.0) license, which permits others to distribute, remix, adapt, and build upon this work for commercial use.

## References

- Entezari M, Ehrampoush MH, Rahimdel A, et al. Is there a relationship between homes' Radon Gas of Ms And Non-Ms individuals, and the patients' paraclinical magnetic resonance imaging and visually evoked potentials in Yazd-Iran?. *Environ Sci Pollut Res Int*. 2021; 28, 8907–14
- Nikosfat M ea. investigation and determination of the amount of thoron( $^{220}\text{Rn}$ ) and radon( $^{222}\text{Rn}$ ) and its environmental consequences on water and soil of lake shoorabil, Ardabil. 2022. Available from: file:///C:/Users/admin/Downloads/6671393h01324[cited Aug 15, 2022].
- Kashkinbayev Y, Kazhiyakhmetova B, Altaeva N, et al. Radon exposure and cancer risk: assessing genetic and protein markers in affected populations. *Biology*. 2025;14(5):506.
- Danforth JM, Provencher L, Goodarzi AAJFiC, et al. Chromatin and the cellular response to particle radiation-induced oxidative and clustered DNA damage. *Front Cell Dev Biol*. 2022;10:910440.
- Asadi Mohammad Abadi A, Rahimi M, Jabbari-Koopaei L. Measurement of dissolved radon concentration in groundwater samples of Shahre Babak city and estimation of annual effective absorbed dose. *Journal of Radiation Safety and Measurement*. 2020;9 (3):31-8.
- Jamir S, Sahoo B, Mishra R, et al. A case study on seasonal and annual average indoor radon, thoron, and their progeny level in Kohima district, Nagaland, India. *Isotopes Environ Health Stud*. 2023;59(1):100-11.
- Rahimi M, Abadi AAM, Koopaei LJJAR, et al. Radon concentration in groundwater, its relation with geological structure and some physicochemical parameters of Zarand in Iran. *Applied Radiation and Isotopes*. 2022;185: 110223.
- Alharbi WR, Abbady AG, El-Taher AJASRJETS. Radon concentrations measurement for groundwater using active detecting method. *American Scientific Research Journal for Engineering, Technology, and Sciences*. 2015;14:1-11.
- Manawi Y, Ahmad A, Subeh M, et al. Evaluation of the Radon Levels in the groundwater wells of Qatar: radiological risk assessment. *Water*. 2023; 15(22):4026.
- Hassanzadeh Reza ea. Analysis of the risk of earthquakes in Kerman city with an emphasis on the use of GIS in preliminary microzoning grade 2. *Geosciences*. 2019;21(81):23-30. Available from: file:///C:/Users/admin/Downloads/55413908103[cited Jun 10, 2019].
- Bortey-Sam N, Nakayama SM, Ikenaka Y, et al. Health risk assessment of heavy metals and metalloid in drinking water from communities near gold mines in Tarkwa, Ghana. *Environ Monit Assess*. 2015;187:1-12.
- Esmail Z, Vali S, Hossein F, et al. Risk assessment of different units in brake pads manufacture by using Frank Morgan method. 2014.
- Malakootian M, Mohammadi A, Faraji M. Investigation of physicochemical parameters in drinking water resources and health risk assessment: a case study in NW Iran. *Environ Earth Sci*. 2020;79(9):195.
- Pourtaghi GH, Bahrami A, Shaban I, et al. Exposure risk assessment of formaldehyde in four military hospitals in Tehran. *Journal of Occupational Hygiene Engineering*. 2020;7(1):21-30.
- Partani S, Rashidi A, Jarahi H, et al. Evaluation of the ecological risk of heavy metals in the sediments of coastal wetlandsCase study:

- coastal wetlands of Chabahar Bay, mangrove ecosystem. *Iranian Journal of Soil and Water Research*. 2024;54(11):1733-57.
16. Mehrabi A. Measuring the concentration of radon gas in groundwater of Jiroft plain and its relation with the region faults. *Journal of Natural Environmental Hazards*. 2019;8(21):267-82.
  17. Rahimi M, Asadi Mohammad Abadi A, Jabbari KL. The measurement of Radon Gas dissolved in groundwater and determination of annual effective absorbed dose of radon gas in Zarand city in 2016. 2018;16(12):1126-37.
  18. Ullah F, Muhammad S, Ali WJC. Radon concentration and potential risks assessment through hot springs water consumption in the Gilgit and Chitral, Northern Pakistan. *Chemosphere*. 2022;287: 132323.
  19. Mousavi Aghdam M, Crowley Q, Rocha C, et al. A study of natural radioactivity levels and radon/thoron release potential of bedrock and soil in southeastern Ireland. *Int J Environ Res Public Health*. 2021;18(5):2709.
  20. Malakootian M, Salmani MH. Determination of radon level in drinking water in Mehriz villages and evaluation the annual effective absorbed dose. 2015.
  21. Negarestani A, Hashemi SM, Naseri F, et al. Preliminary investigation of the variation of Radon concentration in the Jowshan hot spring in the SE of Iran as a precursor for the M 4.9 Shahdad and M 4.3 Sirch earthquakes on May, 2009. 2012;6(2):30-9.
  22. Fakhri MS, Asghari Moghaddam A, Najib M, et al. Investigation of nitrate concentrations in groundwater resources of Marand plain and groundwater vulnerability assessment using AVI and GODS methods. *J Environ Stud (Northborough)*. 2015;41(1):49-66.
  23. Danai Z ea. Evaluation of absorbed dose due to alpha and gamma radiations of radon gas daughter nuclei in tracheal tissue. *Scientific Research Journal of Sabzevar University of Medical Sciences*. 2019;27 (5):612-03. Available from: [https://jsums.medsab.ac.ir/article\\_1343.html?lang=en](https://jsums.medsab.ac.ir/article_1343.html?lang=en) [cited Des 11, 2019].
  24. Mohammad Jafari. Zoning the concentration and ecological risk of heavy metals in the sediments of Mighan lagoon. *Ecohydrology*. 2016;4(2):545-33.
  25. Sehrani M B, Boudaqqpour S, Mirmohammadi M, et al. Radon Gas concentration measurement and assessment of health risk in Tehran, Iran. *Amirkabir Journal of Civil Engineering*. 2019;51(1): 109–18.
  26. Goli Ahmedabad F ea. Estimation of annual effective dose and excess risk of cancer caused by natural gamma near the hot spring. *Jundishapur Medical Scientific Journal*. 2017;17 (3):345-0. Available from: [https://jsmj.ajums.ac.ir/article\\_73463.html?lang=en](https://jsmj.ajums.ac.ir/article_73463.html?lang=en) [cited Feb 11, 2017].